Importance of the D and E Helices of the Molecular Chaperone DnaK for ATP Binding and Substrate Release†

Sergey V. Slepenkov,‡ Brandi Patchen,‡ Kenneth M. Peterson,§ and Stephan N. Witt*,‡

Departments of Biochemistry and Molecular Biology and Microbiology and Immunology, Louisiana State University Health Sciences Center, 1501 Kings Highway, Shreveport, Louisiana 71130-3932

Received January 22, 2003; Revised Manuscript Received March 26, 2003

ABSTRACT: The C-terminal domain of the molecular chaperone DnaK is a compact lid-like structure made up of five α-helices (αA−αE) (residues 508−608) that is followed by a 30-residue disordered, flexible region (609−638). The lid encapsulates the peptide molecule bound in the substrate-binding domain, whereas the function of the 30-residue disordered region is not known. By sequentially deleting the flexible subdomain and the individual lid helices, we deduced the importance of each structural unit to creating long-lived DnaK−peptide complexes. Here we report that (i) the αD helix is essential for long-lived DnaK−peptide complexes. For example, ATP triggers the dissociation of a acrylodan-labeled p5 peptide (ap5, a-CLLLSAPRR) from wtDnaK and DnaK595(A−D) with k_{off} equal to 7.6 and 8.9 s^{-1}, respectively, whereas when the D-helix is deleted, creating DnaK578(A−C), k_{off} jumps to 207 s^{-1}. (ii) The presence of the αB helix impacts the rate of the ATP-induced high-to-low affinity conformational change. For example, ATP induces this conformational change in a lidless variant, DnaK517(1/2A), with a rate constant of 442 s^{-1}, whereas, after adding back the B-helix (residues 518−554), ATP induces this conformational change in DnaK554(A−B) with a rate constant of 2.5 s^{-1}. Our interpretation is that this large decrease occurs because the B-helix of the DnaK554(A−B) is bound in the substrate-binding site. (iii) The deletion analysis also revealed that residues 596−638, which comprise the αE helix and the flexible subdomain, affect ATP binding. Our results are consistent with this part of the lid producing conformational heterogeneity, perhaps by binding to the ATPase domain.

The *Escherichia coli* 70-kDa molecular chaperone DnaK folds, transports, and assembles other proteins in an ATP-dependent activity cycle that is regulated by the cochaperones, GrpE and DnaJ (*1*−*3*). DnaK cycles from an ADP-bound, high-affinity state that tightly binds unfolded substrate to an ATP-bound, low-affinity state that weakly binds substrate. GrpE is the nucleotide exchange factor that catalyzes the release of ADP from ADP−DnaK complexes (*4*−*6*). ADP release in turn permits ATP binding which induces the high-to-low affinity transition. DnaJ promotes the reverse transition (*7*, *8*).

DnaK is composed of three domains: the ATPase domain, the substrate-binding domain, and the lid comprise residues 1−388, 389−508, and 509−638, respectively. The ATPase domain is a bilobed structure that contains a deep channel between the two lobes (*9*, *10*); nucleotide binds at the base of the channel. The substrate-binding domain consists of a uniquely folded β-sandwich subdomain followed by an α-helical domain that consists of five antiparallel α-helices (Figure 1A) (*11*, *12*). This α-helical domain is like a lid over the β-sandwich subdomain (*12*). A network of hydrogen bonds and a salt bridge links the lid noncovalently to the β-sandwich. The bound peptide interacts with the β-sandwich but not the lid (*12*).

The role of the lid in the chaperone activity cycle is still not precisely understood. Interdomain coupling occurs in the absence of the lid (*13*, *14*), although ATP-induced peptide dissociation is significantly accelerated (*15*) compared to the wild-type protein. The 33 C-terminal residues of DnaK, which constitutes a flexible, mobile region of the protein, has no known function (*16*). There are intriguing hints that the lid region of DnaK and other Hsp70s interacts with DnaJ (*17*).

Recent experiments have shown that deletion of the bulk of DnaK's lid, residues 518−638, increases the rate of ATP-induced peptide release from 7.6 to 299 s^{-1} (*18*). Intrigued by this finding, and to determine the relative importance of each helix to peptide release, we have undertaken a study in which the five helices that constitute DnaK's lid plus the 30-residue flexible tail were sequentially deleted. Each variant was then tested for a variety of activities, viz., ATP-induced peptide dissociation, ATP hydrolysis, and the ATP-induced high-to-low affinity conformational change. We show that the αE and αD helices are key helices for lid stability. The αD helix is the key helix with respect to peptide release because when this helix is deleted the rate constant for ATP-induced peptide release jumps from 7.6 to 207 s^{-1}. A model is proposed for how αD stabilizes the lid and creates long-lived DnaK−peptide complexes.

† This work was supported by a grant from the National Institutes of Health (GM 51521) (to S.N.W.).

* To whom correspondence should be addressed. Tel: (318) 675−7891. FAX: (318) 675−5180. E-mail: switt1@ lsuhsc.edu.

‡ Departments of Biochemistry and Molecular Biology.

§ Microbiology and Immunology.

10.1021/bi034126v CCC: $25.00
Published on Web 04/23/2003

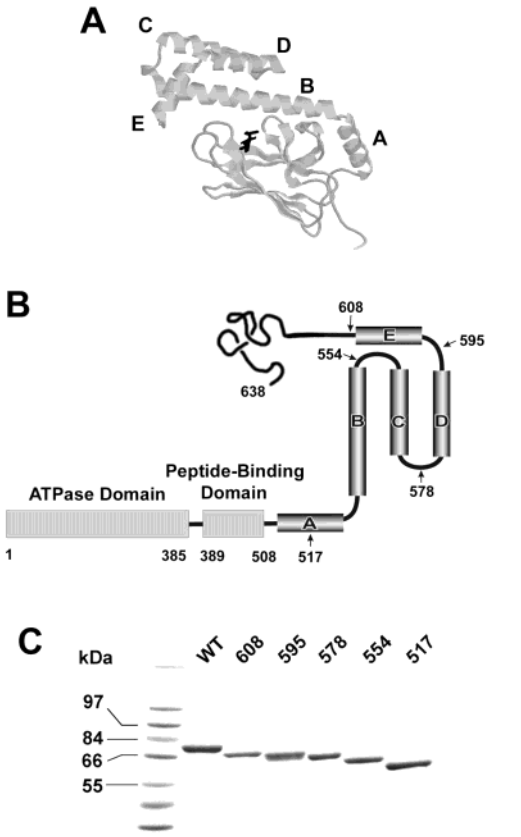

FIGURE 1: (A) Structure of the substrate-binding domain of DnaK (residues 394−607) (*12*). The bound peptide (NRLLLTG) is depicted in black. The five α-helices that comprise the lid are labeled A−E. The image was constructed from PDB file 1DKX. (B) Schematic showing the domains of DnaK. The lid region is not drawn to scale. (C) SDS−PAGE analysis of wild type and the various truncation proteins.

MATERIALS AND METHODS

Protein and Reagents. All reagents were of the highest purity and were purchased from Sigma, unless stated otherwise. Wild-type DnaK and the C-terminal truncation variants were isolated using ATP−agarose affinity chromatography followed by ion exchange chromatography, as described (*19*). The sample buffer consisted of 25 mM *N*-(2-hydroxyethyl) piperazine-*N*′-2-ethanesulfonic acid (HEPES[1])/50 mM KCl/5 mM $MgCl_2$/5 mM 2-mercaptoethanol at pH 7.0. Each protein was made nucleotide-free by either exhaustive dialysis (*20*) or the method of Gao et al. that employs 5′-adenylyl imidodiphosphate (AMP−PNP) (*21*) and then stored in the HEPES sample buffering containing 10% glycerol at −80 °C prior to use. Glycerol was removed by an overnight dialysis before using the protein.

Peptides were purchased from Genemed Synthesis Incorporated (S. San Francisco, CA), purified to >95% by high performance liquid chromatography, and peptide mass was verified by electrospray mass spectroscopy. Acrylodan was covalently attached to the cysteine sulfur atom of the p5 peptide (CLLLSAPRR) and subsequently purified as described (*22*, *23*). The acrylodan−p5 peptide is referred to as ap5. The mass of ap5 was verified by electrospray mass spectrometry. Control experiments showed that unlabeled p5 competitively inhibits the binding of ap5 to DnaK.

Construction of the DnaK Expressing Plasmids. The pMSK plasmid harboring the wild type *dnaK* gene behind an IPTG inducible promoter was a gift to us from Dr. Lila Gierasch (University of Massachusetts, Amherst). Using the QuikChange Site-Directed Mutagenesis kit (Stratagene), a stop codon was introduced into the *dnaK*$^+$ gene such that translation terminates at residue 517 (*18*). This same protocol was used to prepare the C-terminal truncation variants DnaK608(A−E), DnaK595(A−D), DnaK578(A−C), and DnaK554(A−B). Note that DnaK608(A−E) indicates a DnaK variant that possesses the αA through the αE lid helices, and so on for the other variants. The forward (F) and reverse primers (R) used in the PCR reactions were *dnaK*(1−608): F, 5′-CAG CAA CAT GCC TAG CAG CAG ACT GCC-3′ and R, 5′-GGC AGT CTG CTG CTA GGC ATG TTG CTG-3′; *dnaK*(1−595): F, 5′-CTG GCA CAG GTT TGA CAG AAA CTG ATG-3′ and R, 5′-CAT CAG TTT CTG TCA AAC CTG TGC CAG-3′; *dnaK*(1−578): F, 5′-ACT GCT CTG AAA TGA GAC AAA CTG CCG-3′ and R, 5′-CGG CAG TTT GTC TCA TTT CAG AGC AGT-3′; *dnaK*(1−554): F, 5′-GTT GAA GAA GCA TGA GAC AAA CTG CCG-3′ and R, 5′-CGG CAG TTT GTC TCA TGC TTC TTC AAC-3′. Primers were purchased from MWG Biotech, Inc. (High Point, NC).

To ensure that secondary mutations were not introduced during the PCR protocol, the allele for each truncation protein was sequenced at MWG Biotech. The various truncation proteins were expressed in the DnaK-deficient *E. coli* strain BB1553 (*24*) and purified using the same methods as the wild-type protein. N-terminal sequencing (Macromolecular Structure Analysis Facility, University of Kentucky, Lexington) revealed that the start methionine is absent from the wild-type protein and from the C-terminal truncation variants.

SDS−PAGE. WtDnaK and its C-terminal truncation variants were visualized using discontinuous pH sodium dodecyl sulfate−polyacrylamide gel electrophoresis (*25*). The lower and upper gels contained 10 and 5% acrylamide, respectively. Samples of DnaK (20 μL) were boiled for 3 min in the presence of gel loading buffer prior to loading onto the gel. A total of 1.5 μg of protein was loaded per well. Coomasie Brilliant Blue was used to stain the gel.

Stopped-Flow Fluorescence. A SX-18MV stopped-flow fluorescence spectrometer (Applied Photophysics Ltd., Leatherhead, U.K.) was used to monitor spectral changes that occur in the forward and reverse reactions. The dead-time of the instrument was 1.5 ms, and the dimensions of the optical cell where mixing and detection occurs equaled 1 × 0.2 × 0.1 cm. The conditions under which the several different types of rapid kinetic experiments were the same as previously described (*26*). For most stopped-flow experiments, the instrumental time constant was equal to 0.5−1% of the reaction half-time. For the case of very fast reactions, no in-line filtering was used. Each stopped-flow trace is the average of 4−10 individual traces. In some cases, data were collected using a split time base mode. Temperature control of both the jacketed reactants and the jacketed mixing chamber was achieved with a circulating external water bath ($\Delta T = \pm 0.2$ °C). The concentrations in the text refer to after mixing.

[1] Abbreviations: HEPES, *N*-(2-hydroxyethyl) piperazine-*N*′-2-ethanesulfonic acid; acrylodan, a, 6-acryloyl-2-(dimethylamino)naphthalene; p5, the synthetic peptide CLLLSAPRR; ap5, the acrylodan-labeled p5 peptide.

The preparation of preformed DnaK554−ap5 and DnaK578−ap5 complexes was complicated by the presence of the lid binding to the substrate-binding site. For example, for wild type (or DnaK608 or DnaK595 or DnaK517) an excellent signal change occurred on mixing a volume of 1−3 μM protein and 0.5 μM ap5 with an equal volume of 25 μM p5 and 0.02−16 mM ATP. In contrast, to obtain an adequate signal change when using DnaK554 or DnaK578, the concentrations of protein and ap5 peptide were increased significantly. In these cases, mixing 10 μM protein and 5 μM ap5 with an equal volume of 100 μM p5 and 16 mM ATP yielded a reasonable signal change. Because the lid and added peptide compete for binding to DnaK, by mass action, increasing the concentration of the ap5 peptide increases the concentration of the DnaK−ap5 complexes. Because so much ap5 peptide must be used to prepare DnaK554−ap5 and DnaK578−ap5 complexes, for these two variants plots of k_{obs}^{off} versus ATP concentrations were not made. Dissociation was examined only at large, near saturated concentrations of ATP.

ATPase Activity Measured Under Single Turnover Conditions by Fluorescence Spectroscopy. A Photon Technology Inc. (So. Brunswick, NJ) StrobeMaster lifetime spectrometer with a SE−900 steady state fluorescence option was used to measure the slow, single-exponential increase in tryptophan fluorescence that occurs as DnaK hydrolyzes ATP under single turnover conditions ([DnaK] = [ATP]). It has been shown previously (*20*) that the first-order rate constant for this slow increase in tryptophan fluorescence equals the rate constant for DnaK-catalyzed ATP hydrolysis. The excitation source was a 75-watt xenon arc lamp, and the detection was accomplished with a photon counting detector (PTI model 710). Solutions of DnaK were maintained in a quartz cuvette (1-cm path length) with constant stirring and temperature control via an external circulating heating/cooling bath ($\Delta T = \pm 0.2$ °C). A substoichiometric amount of ATP was added to the cuvette, and the increase in tryptophan fluorescence was monitored in the time base mode, with $\lambda_{ex} = 295$ (3 nm bandwidth) and $\lambda_{em} = 340$ nm (5 nm bandwidth). Sample temperature was verified using a hand held thermocouple, which was placed directly into the sample.

Curve Fitting. Stopped-flow data were fitted to single-exponential function using a curve fitting program that used a Marquardt algorithm based on the program Curfit given in Bevington (*27*). Least-squares fitting of data to hyperbolic or linear equations and determinations of standard errors of the fitted parameters were conducted using the program KaleidaGraph (Synergy Software, Reading, PA).

RESULTS

Stopped-flow studies have yielded many insights into the mechanism of the interaction of DnaK with ATP and peptides. One type of experiment is where ATP is mixed with a solution of DnaK−fluorescent peptide complexes and changes in fluorescence upon dissociation of the tagged peptide are monitored. Another type of experiment is where ATP is mixed with a solution of DnaK or DnaK−peptide complexes and changes in DnaK's tryptophan fluorescence upon ATP binding are monitored. In the latter case, it is convenient that DnaK possesses only one tryptophan residue, W102 (*28*). Both types of experiments are conducted in this study.

We previously found that DnaK's lid, residues 518−638, has a huge impact on the kinetics of ATP-triggered peptide release (*18*). For example, ATP triggers the release of the ap5 peptide from preformed wtDnaK−ap5 complexes with a first-order rate constant of ~8 s^{-1}, whereas upon deletion of the lid ATP triggers the release of ap5 from preformed DnaK517−ap5 complexes with a first-order rate constant of 299 s^{-1}. Other effects are that ATP binds to wtDnaK in two discrete phases, as judged by tryptophan fluorescence quenching, but to DnaK517 in only one phase (*20*, *26*). To dissect the residues that are responsible for creating long-lived DnaK−peptide complexes, and to uncover why ATP binds to wtDnaK in two phases but to DnaK517 in only one phase, we created a series of DnaK deletion variants. First we deleted the flexible region, creating DnaK608(A−E), and then sequentially deleted each lid helix (DnaK608(A−E) → DnaK595(A−D) → DnaK578(A−C) → DnaK554(A−B) → DnaK517(1/2A).

A schematic of the C-terminal domain of DnaK, with truncation points indicated, is shown in Figure 1B. SDS−PAGE analysis of wild type DnaK and its variants show that DnaK migrates progressively faster through the gel as the lid helices are removed (Figure 1C). Rapid mixing experiments were then conducted on all five C-terminal truncation variants of nucleotide-free DnaK, in the absence of added peptide, as described below.

Effect of the Sequential Deletion of the Lid Helices on the ATP-Induced Conformational Change. Figure 2 compares ATP-induced quenching of tryptophan fluorescence in wtDnaK, DnaK608, and DnaK595. For the wt protein, ~50% of the ATP-induced tryptophan quenching occurs in a rapid phase ($k_{obs,1} = 19 \pm 1$ s^{-1}) and ~50% in a slow phase ($k_{obs,2} = 0.62 \pm 0.03$ s^{-1}). When the 30 residues that make up the disordered region of the C-terminus are deleted (DnaK608), ~70% of the ATP-induced quenching occurs in a rapid phase ($k_{obs,1} = 37 \pm 1.4$ s^{-1}) and ~30% in a slow phase ($k_{obs,2} = 4.5 \pm 0.3$ s^{-1}). Interestingly, when the αE helix is deleted (DnaK608 → DnaK595) ATP binding quenches the tryptophan fluorescence of DnaK595 in a single phase ($k_{obs} = 1.83 \pm 0.02$ s^{-1}). ATP binding also quenches the tryptophan fluorescence of DnaK578, DnaK554, and DnaK517 in a single phase (Table 1). The results reveal something quite unexpected: the disordered subdomain (residues 609−638) and the αE helix (residues 596−608) modulate the kinetics of ATP binding. In the discussion section, we posit that the 30-residue flexible tail of DnaK interacts with the ATPase domain, and that this interaction causes heterogeneity, which in turn affects ATP binding.

Following the above initial characterization, to understand how the lid modulates ATP binding to DnaK, we conducted a detailed kinetic analysis of the reaction between ATP and the various truncation proteins. The experiments consisted of varying the concentration of ATP at a fixed concentration of DnaK, with the stipulation that [ATP] ≫ [DnaK]. Figure 3 A shows representative stopped-flow traces obtained upon mixing 2 μM nucleotide-free DnaK595 with ATP. Traces obtained over a wide range of ATP concentrations follow single-exponential kinetics. The traces, obtained at 5 and 320 μM ATP, exhibit observed first-order rate constants equal to 0.56 ± 0.01 and 1.99 ± 0.01 s^{-1}, respectively. Figure 3B

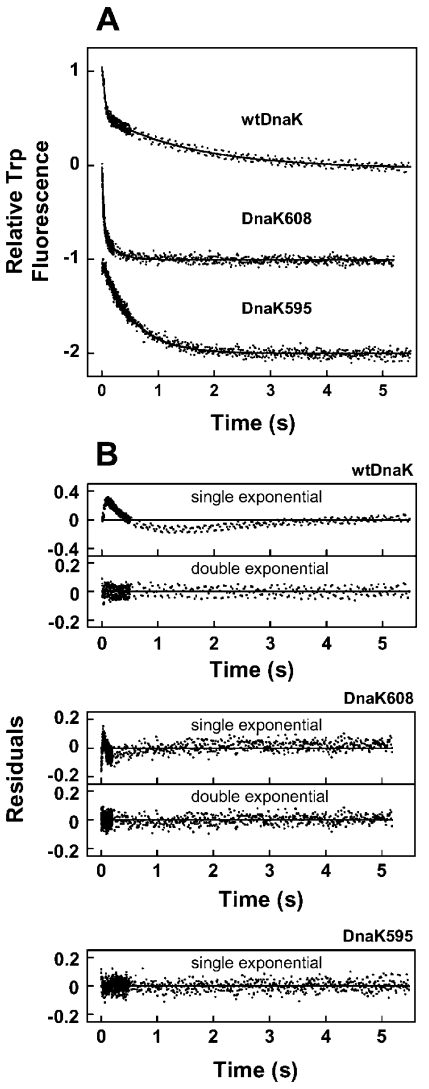

FIGURE 2: Comparison of ATP-induced quenching of tryptophan fluorescence in wild type, DnaK608, and DnaK595 (A). (B) Residuals from single- and double-exponential fits. For the wt protein, ATP-induced quenching occurs in two phases of nearly equal amplitude. For DnaK608 70% of the ATP-induced quenching occurs in the rapid phase and 30% in the slow phase. In contrast, for DnaK595 ATP binding quenches the tryptophan fluorescence of the protein in a single phase. Rate constants are given in the text and Table 1. Conditions: protein concentration was 1 μM; ATP was at saturating concentrations, 1 and 0.32 mM for wtDnaK and the two variants, respectively. Concentrations refer to after mixing. Temperature = 25 °C.

shows a plot of k_{obs} versus [ATP]. The hyperbolic nature of the plot is consistent with the following two-step sequential reaction (*26*).

$$\mathrm{ATP} + \mathrm{DnaK595} \overset{K' = 11\ \mu\mathrm{M}}{\rightleftharpoons} \mathrm{ATP{-}DnaK595} \overset{k_2 = 2.1\ \mathrm{s}^{-1}}{\underset{k_{-2} \ll k_2}{\rightleftharpoons}} \mathrm{ATP{-}DnaK595^*} \quad (1)$$

In the above equation, ATP−DnaK595 is an intermediate, ATP−DnaK595* is the low-affinity form of DnaK, and the asterisk denotes reduced tryptophan fluorescence of the ATP−DnaK595* state relative to DnaK595. Using the steady-state approximation, it can be shown that the observed first-order rate constant associated with eq 1 obeys relation 2, with $K_1' = (k_{-1} + k_2)/k_1$.

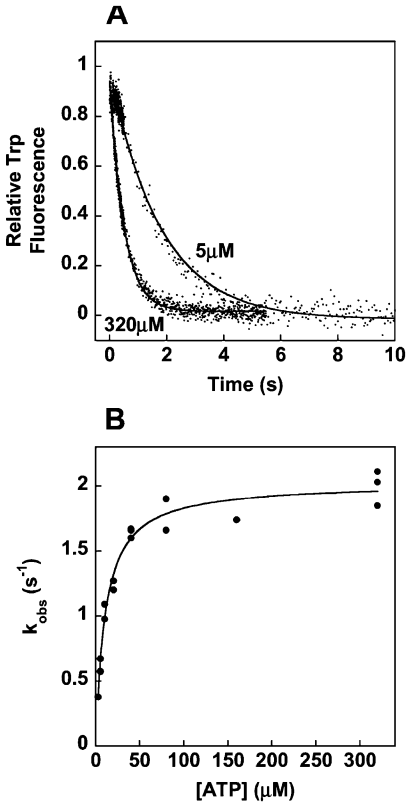

FIGURE 3: Kinetics of ATP-induced quenching of W102 in DnaK595. (A) Stopped-flow traces obtained on mixing nucleotide-free DnaK595 with ATP. Solid lines are the fits to a single-exponential function ($F(t) = \Delta F e^{-k_{obs}t} + F_\infty$) Concentrations before mixing: 2 μM DnaK595 and 10 or 640 μM ATP; k_{obs} equals 0.56 ± 0.01 s^{-1} (5 μM ATP) and 1.99 ± 0.01 s^{-1} (320 μM ATP). (B) Plot of k_{obs} versus [ATP]. Data are fit to $k_{obs} = k_{-2} + k_2[\mathrm{ATP}]/(K_1' + [\mathrm{ATP}])$ (solid line), yielding k_2 (asymptote) = 2.1 ± 0.2 s^{-1}, k_{-2} (y-intercept) = −0.01 ± 0.17 s^{-1}, and K_1' = 11 ± 3 μM.

$$k_{obs} = k_{-2} + \frac{k_2[\mathrm{ATP}]}{K_1' + [\mathrm{ATP}]} \quad (2)$$

According to eq 2, the asymptote of the plot of k_{obs} versus [ATP] (Figure 3B) equals $k_2 + k_{-2}$; the y-intercept equals k_{-2}; and the ATP concentration that gives half-maximal response equals K_1' (*29*). Because the y-intercept ≈ 0 indicates that $k_2 \gg k_{-2}$; thus, the asymptote of the plot approximates k_2. For DnaK(2−595), the parameters k_2 and K_1' are 2.1 ± 0.2 and 11 ± 3 μM, respectively. The other truncation proteins, DnaK578, DnaK554, and DnaK517, also display a hyperbolic dependence of k_{obs} (for ATP-induced tryptophan decrease) versus [ATP]. The kinetic constants for those variants are given in Table 1.

Inspection of Table 1 (left panel) shows that k_2 equals 442 s^{-1} for DnaK517, and then decreases precipitously to ∼2.1−2.5 s^{-1} for DnaK554, DnaK578, and DnaK595. Our interpretation of the precipitous decrease in k_2 upon the addition of lid residues to DnaK517 hinges on an NMR study of Wang and co-workers, who showed that the B-helix of the DnaK fragment 389−561 is bound in the β-sandwich substrate-binding domain (*30*). The B-helix is most certainly bound in the substrate-binding pocket for the variant DnaK554, and this *cis*-acting ligand, like a *trans*-acting ligand, dramatically stabilizes the conformation of the substrate-binding domain. We suggest that the enhanced

Table 1. Kinetic Constants

DnaK species	tryptophan fluorescence − peptide			acrylodan fluorescence + peptide	
	phases of Trp fluorescence decrease	K_1' (μM)	k_2 (s^{-1})	K_1' (μM)	k_2 (s^{-1})
wtDnaK	2	*a*	*a*	28 ± 2	7.6 ± 0.5
608 αA−αE	2	*a*	*a*	28 ± 4	7.4 ± 0.2
595 αA−αD	1	11 ± 3	2.1 ± 0.2	29 ± 4	8.9 ± 0.4
578 αA−αC	1	12 ± 1	2.5 ± 0.1	ND	207 ± 17
554 αA−αB	1	8 ± 1	2.5 ± 0.1	ND	208 ± 14
517 $^1/_2$ αA	1	1691 ± 181	442 ± 13	1060 ± 185	299 ± 21

[a] See "Effect of the Sequential Deletion of the Lid Helices on the ATP-Induced Conformational Change." ND, not determined. Temperature = 25 °C.

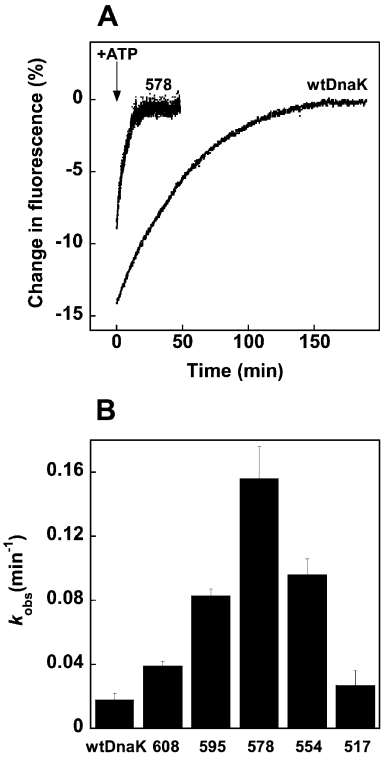

FIGURE 4: Single turnover ATPase fluorescence assay. (A) A rapid reduction in fluorescence occurred upon the addition of ATP to DnaK ([ATP] = [wtDnaK] or [DnaK578] = 1 μM). The subsequent slow increase in fluorescence follows the equation $F(t) = \Delta F(1 - \exp(-k_{obs}t)) + \gamma$ (solid lines), where ΔF, k_{obs}, and γ are the amplitude, the first-order observed rate constant, and the fluorescence at the time zero point, respectively. Best-fit values for k_{obs} are 0.155 and 0.019 min^{-1} for DnaK578 and wtDnaK, respectively. Since DnaK-catalyzed ATP hydrolysis occurs at the same rate as the slow increase in fluorescence, $k_{obs} \approx k_{hy}$. Conditions: λ_{ex} = 295 nm (bandwidth = 3 nm); λ_{em} = 340 nm (bandwidth = 5 nm). (B) Plot of k_{hy} versus DnaK species.

rigidity of the substrate-binding site in the presence of the bound lid makes it more difficult for ATP to catalyze the high-to-low conformational transition. Thus, the *cis*-acting ligand retards the rate of the ATP-induced conformational change.

Single Turnover ATPase Experiments. Because added peptides stimulate DnaK-mediated ATP hydrolysis from 4- to 20-fold (*31*, *32*), an internal ligand should also stimulate hydrolysis. Thus, if DnaK554, DnaK578, and DnaK595 exhibit self-binding in the absence of added peptide, then these variants should also exhibit enhanced ATP hydrolysis compared to wild type. To test this hypothesis, the ATPase activity of the various DnaK truncation proteins was measured using the following fluorescence assay. When a substoichiometric amount of ATP is added to a cuvette containing 1 μM DnaK, the tryptophan fluorescence rapidly decreases due to the ATP-induced high-to-low conformational change in the protein, and, as DnaK hydrolyzes ATP this conformational change is slowly reversed, causing the fluorescence to slowly recover. The first-order rate constant, k_{obs}, for this increase in tryptophan fluorescence is identical to the reported rate constant, k_{hy}, for DnaK-mediated ATP hydrolysis (*20*, *33*). Possible mechanisms for the reversal of the high-to-low affinity conformational change have been discussed (*1*, *34*).

Figure 4A shows that the recovery in tryptophan fluorescence occurs much faster for DnaK578 compared to the wild-type protein. Specifically, at 25 °C the first-order rate constant for the recovery of fluorescence is 0.019 and 0.155 min^{-1} for wild type and DnaK578, respectively. The former value agrees with reported values of k_{hy} in the absence of added peptide (*20*, *33*), whereas the 8-fold increase in k_{hy} for DnaK578 is consistent with previously reported values for k_{hy} in the presence of added peptide (*31*, *32*). Figure 4B shows the results for all of the truncation proteins. Interestingly, wtDnaK, DnaK608, and DnaK517, which lacks almost the entire lid, exhibit nearly the same ATPase activity, whereas the other three truncation proteins exhibit a 2−8-fold increase in ATPase activity. Further, we find that the p5 peptide at 200 μM fails to stimulate DnaK578-mediated ATP hydrolysis. These findings support the hypothesis that for DnaK595, DnaK578, and DnaK554 the lid itself binds in the substrate-binding site, and this produces two effects: the rate of the ATP-induced conformational change decreases, and the rate of DnaK-mediated ATP hydrolysis increases.

Effect of the Sequential Deletion of the Lid Helices on the Kinetics of ATP-Induced Peptide Release. The foregoing results led us to examine the effect of deletion of the individual lid helices on ATP-induced peptide dissociation from DnaK. The p5 peptide (CLLLSAPRR), which has been used in numerous kinetic studies (*18*, *35*, *36*), was used. The acrylodan-labeled version of this peptide is ap5. Stopped-flow rapid mixing experiments were then conducted on all six forms of DnaK by varying the concentration of ATP at a fixed concentration of protein. Excess unlabeled p5 peptide was contained in the same syringe as ATP to minimize ap5 rebinding. In this case, peptide dissociation occurs via reaction 3 (*18*). The asterisk indicates decreased fluorescence of the free peptide relative to the bound peptide. Kinetic parameters were extracted from the observed dissociation rate constants using eq 4, which was derived using the steady-

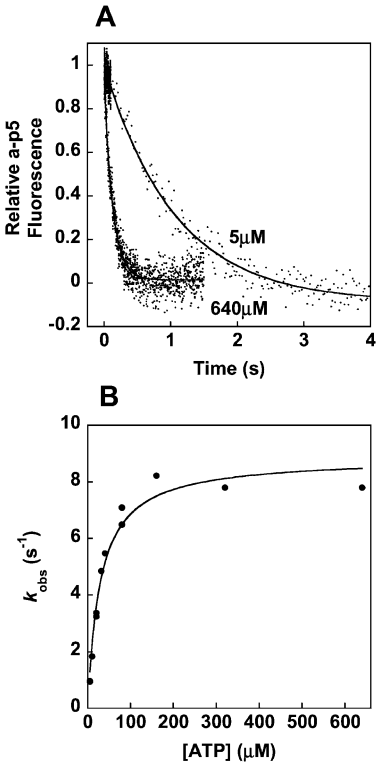

FIGURE 5: ATP-induced peptide release from DnaK595. (A) Stopped-flow traces obtained on mixing nucleotide-free DnaK595−ap5 complexes with ATP. Solid lines are the fits to a single-exponential function ($F(t) = \Delta F e^{-k_{obs}t} + F_\infty$). Concentrations before mixing, where the brackets denote syringes: [3 μM DnaK595 + 0.5 μM ap5] and [25 μM p5 + 10 or 1280 μM ATP]; k_{obs}^{off} equals 0.94 ± 0.02 s^{-1} (5 μM ATP) and 7.8 ± 0.1 s^{-1} (640 μM ATP). (B) Plot of k_{obs}^{off} versus [ATP]. Data are fit to $k_{obs}^{off} = k_2[ATP]/(K_1' + [ATP])$ (solid line), yielding $k_2 = 8.9 \pm 0.4$ s^{-1}, and $K_1' = 29 \pm 4$ μM.

$$\text{ATP} + \text{DnaK}-\text{fP} \underset{k_{-1}}{\overset{k_1}{\rightleftharpoons}} \text{ATP}-\text{DnaK}-\text{fP} \xrightarrow{k_2} \text{ATP}-\text{DnaK} + \text{fP}^* \quad (3)$$

state approximation.

$$k_{obs}^{off} = \frac{k_2[ATP]}{K_1' + [ATP]} \quad (4)$$

Representative ap5 dissociation traces for the DnaK595 variant are shown in Figure 5A. Over a wide range of ATP concentrations, the traces follow single-exponential kinetics. The observed first-order rate constants for the traces obtained at 5 and 640 μM ATP equal 0.94 ± 0.02 and 7.8 ± 0.1 s^{-1}, respectively. A plot of k_{obs}^{off} versus [ATP] is shown in Figure 5B. The data are fit to eq 4, yielding values for k_2 and K_1' of 8.9 ± 0.4 s^{-1} and 29 ± 4 μM, respectively. For comparison, values for these two parameters for the other truncation variants and for the wild-type protein are given in Table 1.

Inspection of the ATP-induced peptide off-rate constants in Table 1 reveals a novel finding: Deletion of the αD from DnaK595, which results in DnaK578, causes a 23-fold increase in the rate of ATP-induced peptide release (8.9 → 207 s^{-1}). Peptide dissociation traces for these two variants are shown in Figure 6. A more modest increase in the rate of ATP-induced peptide release occurs upon deletion of the αB (208 → 299 s^{-1}). The dissociation experiments demonstrate that the D-helix, residues 579−595, is absolutely required for long-lived DnaK−peptide complexes.

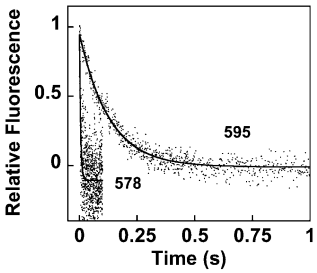

FIGURE 6: Deletion of αD accelerates peptide dissociation. Stopped-flow traces obtained on mixing nucleotide-free DnaK595−ap5 complexes or DnaK578 with ATP. Solid lines are the fits to a single-exponential function ($F(t) = \Delta F e^{-k_{obs}t} + F_\infty$). Concentrations before mixing, where the brackets denote syringes: DnaK595, [3 μM DnaK595 + 0.5 μM ap5] and [25 μM p5 + 16 mM ATP]; DnaK578, [10 μM DnaK578 + 5 μM ap5] and [100 μM p5 + 16 mM ATP]; and k_{obs}^{off} equals 7.8 ± 0.1 and 207 ± 16 s^{-1} for DnaK595 and DnaK578, respectively.

DISCUSSION

This C-terminal deletion analysis of DnaK revealed that the flexible region influences the kinetics of ATP binding to wtDnaK, deletion of the αE helix triggers internal ligand formation, and that the αD helix is required for long-lived DnaK−peptide complexes. We seek below to integrate this new information into our thinking about how ATP interacts with DnaK.

Lid Helices and Internal Ligand Formation. This report revealed the dramatic effect of adding lid helices αB−αE to DnaK517 on the kinetic parameter k_2 and the ATPase activity. Our interpretation is that the truncated lid is an internal ligand in the variants DnaK554, DnaK578, and DnaK595. The basis for this interpretation is the work of Wang and colleagues (*30*). They were the first to show that internal ligand formation, i.e., self-binding, occurs in DnaK(386−561), which is a fragment that contains the β-sandwich substrate-binding domain plus the lid helices αA and αB. Their work revealed that the C-terminal part of αB unwinds, commencing at residue 537, and lodges, intramolecularly, in the substrate-binding pocket. The sequence of αB that actually binds in the pocket is ^{540}DHLLHSTR^{547}. Apparently, the side chain of the second leucine residue, L543, and only this second residue, is tightly held in a deep hydrophobic within the substrate-binding site. A reasonable conclusion is that, given the similarity of DnaK(386−561) to the C-terminal portion of DnaK554), the αB helix of DnaK554 also binds in the substrate-binding pocket. Our results are consistent with self-binding, because adding back the αB helix to DnaK517 dramatically (i) decreases the rate of the ATP-induced high-to-low affinity conformational change due to stabilization of the β-sandwich domain (k_2: 442 → 2.5 s^{-1}) (Table 1); (ii) stimulates the ATPase activity of DnaK554, compared to both DnaK517 and the wild-type protein (k_{hy}: 0.03 → 0.09 min^{-1}) (Figure 4B); and (iii) reduces peptide binding compared to wild type (and even to DnaK517). Because DnaK578 and DnaK595 exhibit similar activities as DnaK554, we conclude that the lid of these two variants is also bound in the substrate-binding site via the unraveled αB helix.

It is interesting to examine what segment of the lid abolishes internal ligand formation. Recall that ATP binds to nucleotide-free DnaK595 in a single phase with k_2 equal to 2.1 s^{-1}. Remarkably, when the short αE helix is added back, ATP binds to DnaK608 very much like it does to the wild-type protein, in that there are two phases of ATP-induced fluorescence quenching ($k_{obs,1} = 39$ s^{-1} and $k_{obs,2} = 4.5$ s^{-1}) (Figure 2). Our interpretation is that, in the special case of no added peptide, addition of the αE helix abolishes internal ligand formation (eq 5). And once the 30-residues

$$\text{DnaK595 (lid: unraveled internal ligand)} \xrightarrow{+\alpha E} \text{DnaK608 (lid: helical bundle)} \quad (5)$$

of the flexible domain are added back, i.e., DnaK608 → wtDnaK, ATP binds to the wild-type protein in two phases with $k_{obs,1} = 19$ s^{-1} and $k_{obs,2} = 0.6$ s^{-1}. Comparing the rate constants for ATP binding to DnaK608 and wtDnaK, we see that adding back the tail decreases both $k_{obs,1}$ (39 → 19 s^{-1}) and $k_{obs,2}$ (4.5 → 0.6 s^{-1}). Thus, the 30-residue flexible tail of wtDnaK inhibits ATP binding. On the basis of these results, we conclude that, in the absence of added peptide, the αE helix promotes the formation of the antiparallel helical bundle composed of the B−D helices and prevents internal ligand formation.

Importance of the αD Helix. If the lid of DnaK554, DnaK578, and DnaK595 is unraveled and bound in the substrate-binding domain, then a peptide added in trans to any of these variants should compete with the unraveled αB helix for the substrate-binding pocket and displace αB. With dysfunctional lids, ATP-triggered peptide release from these three complexes should be very fast, perhaps as fast as ATP-triggered release of peptide from the lidless variant, DnaK517. Indeed, ATP-triggered ap5 dissociation is almost as fast from DnaK554 and DnaK578 ($k_2 \approx 208$ s^{-1}) as from DnaK517 ($k_2 = 299$ s^{-1}) (Table 1). Strikingly, ATP-triggered ap5 dissociation from DnaK595 occurs at the same rate as wild type ($k_2 \approx 8$ s^{-1}). The results indicate that the lid forms a compact structure that encapsulates the bound peptide only for DnaK595. The bound peptide orders the substrate-binding site of DnaK595 in such a way that permits helices αA−αD to adopt an antiparallel structure that is latched to the β-sandwich domain (Figure 7 A). Thus, in the case of added peptide, the D-helix is necessary and sufficient to create the protective lid structure. Note that an NMR study of the β-sandwich domain has shown that indeed peptide binding to the β-sandwich domain significantly reduces conformational flexibility in specific strands and loops of the β-domain (*13*).

Hsp70 Reaction Mechanism. A multitude of different methods has been employed to solve the problem of how DnaK and other 70-kDa chaperones utilize ATP. Proteolytic assays (*37*), filter-binding assays (*33*, *38*), small-angle X-ray scattering (*39*, *40*), and stopped-flow techniques (*20*, *41*, *42*) have yielded numerous insights into the interaction between ATP and 70-kDa chaperones. Comparing mechanisms put forth from these diverse studies is often complicated by the fact that some techniques probe equilibrium species, whereas others probe transients. On the other hand, it is quite useful to compare mechanisms derived from studies that employ the same technique.

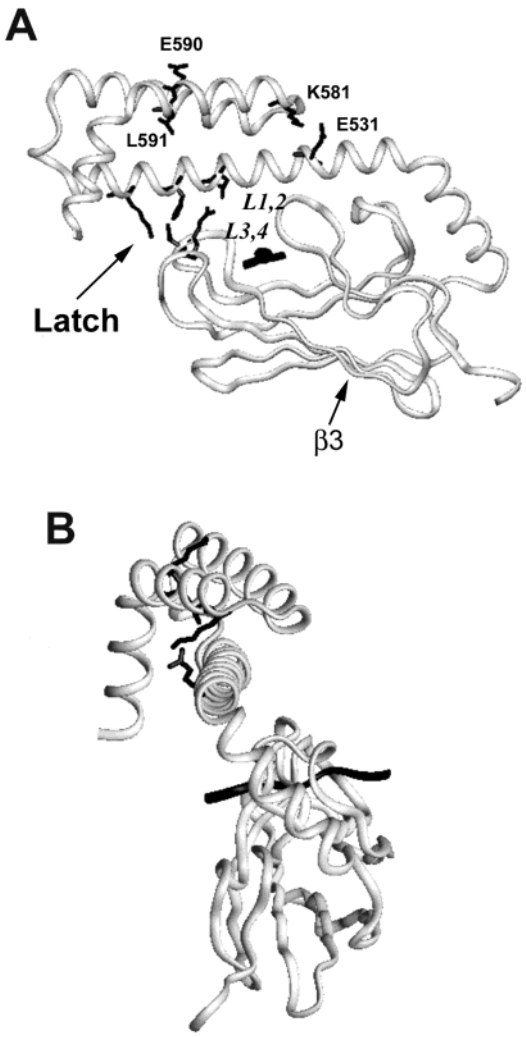

FIGURE 7: Structure of the lid (*12*). (A) Shown are a potential salt-bridge between αB E531 and αD K581, the two conserved residues of the D-helix, E590 and L591, and the interactions that make up the latch. The bound peptide (NRLLLTG) is depicted in black. The image was constructed from PDB file 1DKX. (B) Side view emphasizing the proximity of E531 and K581.

We compare here findings from stopped-flow kinetic studies of ATP binding to bovine brain Hsc70 and ATP binding to DnaK. When ATP binds to nucleotide- and peptide-free Hsp70 or Hsc70 two phases of tryptophan fluorescence quenching occur (*20*, *35*, *41*). But there are subtle differences in the kinetics of ATP binding to these two chaperones that warrant further discussion (*1*).

For bovine brain Hsc70, the observed rate of the rapid phase of ATP-induced fluorescence quenching is a *linear* function of ATP concentration, whereas the observed rate of the slow phase exhibits almost no dependence on ATP concentration (*41*). Such results are consistent with the following two-step mechanism (*43*). In the above reaction,

$$\text{ATP} + \text{Hsc70} \rightleftharpoons \text{ATP}-\text{Hsc70}^* \rightleftharpoons \text{ATP}-\text{Hsc70}^{**} \quad (6)$$

the asterisk denotes decreased tryptophan fluorescence relative to Hsc70, and F(Hsc70) > F(ATP−Hsc70*) > F(ATP−Hsc70**) (F stands for fluorescence). Unfortunately, the effect of added peptide on the kinetics of ATP binding to Hsc70 was never examined.

In contrast, for DnaK, the observed rate of the rapid phase of ATP-induced tryptophan fluorescence quenching exhibits

a *hyperbolic* dependence on ATP concentration, with an asymptote equal to 15−19 s^{-1}, whereas the observed rate of the slow phase (0.5 − 0.7 s^{-1}) exhibits almost no dependence on ATP concentration (*20*, *35*). Such results are formally consistent with a linear three-step mechanism (*20*) or a conformational equilibrium that precedes a two-step sequential reaction (eqs 7 and 8) (*26*). We have previously proposed

$$_{c}\text{wtDnaK} \overset{\text{slow}}{\rightleftharpoons} {}_{o}\text{wtDnaK} \quad (7)$$

$$\text{ATP} + {}_{o}\text{wtDnaK} \rightleftharpoons \text{ATP}-\text{wtDnaK} \rightleftharpoons \text{ATP}-\text{wtDnaK}^* \quad (8)$$

that the ATPase domain of wtDnaK equilibrates between closed and open conformations (eq 7). ATP binds to the open and not the closed conformation in a two-step sequential reaction in which the ATP-triggered conformational change and a simultaneous decrease in tryptophan fluorescence (denoted by the asterisk) occur in the second step (eq 8). When ATP is mixed with nucleotide- and peptide-free wtDnaK, and [$_{c}$wtDnaK] ≈ [$_{o}$wtDnaK], the rapid phase of ATP-induced tryptophan fluorescence quenching is due to the second step of reaction (*8*), whereas the slow phase of tryptophan fluorescence quenching is due to the closed-to-open transition (eq 7: $_{c}$wtDnaK → $_{o}$wtDnaK). Strikingly, when a peptide is added in trans ATP binds to DnaK−peptide complexes and produces one phase of tryptophan fluorescence quenching (*26*); the apparent first-order rate constant, in this case, exhibits a hyperbolic dependence on ATP concentration. On the basis of these results, we proposed that peptide binding shifts all of the wtDnaK molecules to the open state, and this abolishes the slow phase of ATP binding. Thus, with added peptide, ATP rapidly binds to DnaK−peptide complexes in a two-step mechanism (eq 8).

Heterogeneity and C-Terminal Residues 596−638. Our C-terminal deletion analysis of DnaK revealed that the flexible subdomain (residues 596−638) affects ATP binding (Figure 2). Our interpretation is that residues 596−638 produce conformational heterogeneity, and this heterogeneity results in two phases of ATP binding (because one of the conformers is more reactive than the other toward ATP). We discuss below three mechanisms by which these C-terminal residues can produce heterogeneity.

First, wtDnaK self-associates (*44*). Self-association is probably linked to the presence of the C-terminal flexible domain. Self-association at high DnaK concentrations is the reason why crystals of the full-length protein are so difficult to obtain. Crystals of the substrate-binding domain of DnaK can only be obtained when the flexible domain is deleted (*12*) (Figure 7A). So, the wild-type DnaK exists in a concentration-dependent equilibrium between monomers and dimers (and higher-order species at very high protein concentrations) (eq 9). If monomers and dimers interconvert

$$2\ \text{wtDnaK} \rightleftharpoons \text{wtDnaK}_2 \quad (9)$$

slowly (compared to ATP binding) and exhibit different reactivity toward ATP, then the above equilibrium can account for the biphasic kinetics of ATP binding to wtDnaK. However, notice that (i) wtDnaK is completely monomeric at 0.2 mg/mL at 25 °C (*19*, *44*) and our experiments were conducted at concentrations less than 0.2 mg/mL; (ii) two phases of ATP-induced tryptophan fluorescence quenching, with approximately the same relative amplitudes, are even observed at very low concentrations of wtDnaK (0.007 mg/mL) (Slepenkov & Witt, unpublished results); and (iii) DnaK608, which lacks the 30-residue flexible tail, exhibits two phases of ATP binding. For reasons (i−iii), we conclude that the biphasic kinetics of ATP binding to wtDnaK and DnaK608 is not due to self-association.

Second, suppose that the 30-residue flexible C-terminal region of DnaK binds in the substrate-binding site according to

$$\text{wtDnaK (free flexible domain)} \rightleftharpoons \text{wtDnaK (bound flexible domain)} \quad (10)$$

If the two species interconvert slowly (compared to ATP binding) and exhibit different reactivity toward ATP, then this equilibrium can also account for the biphasic kinetics of ATP binding to wtDnaK. On the other hand, we know that a bound peptide, whether in cis or trans, stimulates DnaK's ATPase activity. If the 30-residue flexible tail is removed (wtDnaK → DnaK608), self-binding can no longer occur, thus the steady-state ATPase activity of DnaK608 should be *less* than wtDnaK. That the ATPase activity of DnaK608 is greater than the ATPase activity of wtDnaK and equal to the ATPase activity of DnaK517 (Figure 4B), which has no *cis*-bound peptide, is inconsistent with the above model. For these reasons, we rule out equilibrium (*10*) as a cause of the biphasic kinetics of ATP binding.

Third, consider the possibility that residues 596−638 bind to the ATPase domain of DnaK, and that the interaction creates a closed-to-open equilibrium in this domain (eq 7).

If the closed and open conformations interconvert slowly (compared to ATP binding) and exhibit different reactivity toward ATP, then ATP will bind in two discrete phases. In support of this hypothesis, evidence exists that the C-terminal flexible domain of the eukaryotic Hsc70 protein binds to the ATPase domain through a regulatory motif (EEVD) (*45*). Interestingly, DnaK possesses an EEV sequence within the flexible 30-residue domain. Because equilibria 9 and 10 are ruled out, heterogeneity, caused by an interaction between the αE helix and the flexible domain with the ATPase domain (eq 7), is the best explanation for the observed biphasic kinetics of ATP binding to DnaK.

It is interesting to examine our kinetic results in the light of NMR studies of the apo β-domain of DnaK (residues 393−507) (*13*). This small fragment contains the β-sandwich domain without the lid. Significant differences were found between the structure of the apo β-domain and the structure of this domain with the binding site occupied by peptide. For the apo β-domain (i), the space where the substrate would bind is partially occluded by loop L3,4 and to a lesser extent by loop L1,2 (these are the two inner loops in Figure 7A); and (ii) significant conformational flexibility, characterized by motions on the millisecond to microsecond time scale, occurs in two of the β-strands (β3 and β6) and in one of the loops (L2,3). In contrast, in the peptide-bound state, (iii) conformational exchange or flexibility associated with strand β3 and with several of the loops disappears; and (iv) peptide binding induces chemical shift changes in residues that are also distant form the binding site. In short, peptide binding significantly reduces conformational flexibility (or heterogeneity) of the β-domain. Our kinetic data also show that

peptide binding eliminates the conformational heterogeneity of the wild-type protein.

Given the significant conformational flexibility of the β-sandwich domain in the peptide-free state, it is reasonable that the peptide-free state of wtDnaK is characterized by substantial conformational flexibility in both the β-sandwich domain and the lid. Perhaps in the peptide-free state the partial occlusion of the substrate-binding site by loops L3,4 and L1,2 prevent the lid from interacting with the β-sandwich via the latch (Figure 7A); instead, in this conformation, the flexible region of the lid interacts with the ATPase domain, resulting in closure of the domain. On the other hand, in a subset of peptide-free wtDnaK molecules the lid probably interacts with the β-domain via the latch (Figure 7A), and in this conformation the lid cannot interact with the ATPase domain. Of course, molecules equilibrate between these two states (eq 7). Adding peptide in trans (or cis) affects this conformational equilibrium because peptide binding orders the β-sandwich domain (*13*). This ordering allows the lid to interact with the β-sandwich domain via the latch, and in this position the lid, we propose, can no longer interact with the ATPase domain.

The possibility that the ATPase domain of DnaK can be open or closed is reinforced by what we know about hexokinase. The ATP plus glucose-binding core of yeast hexokinase is almost identical to the tertiary structure of the ATP-binding core of the N-terminal fragment of Hsc70 (*9*). It is known that hexokinase equilibrates between open and closed conformations in the absence of glucose (*46*). Data from fluorescence temperature-jump experiments that monitored the binding of glucose to dimeric yeast hexokinase P−I were interpreted in terms of a concerted Monod-Wyman-Changeux mechanism that contains a preequilibrium similar to reaction 7 (*47*).

Antibiotics and the α*D and* α*E Helices*. Several recent reports have indicated that DnaK is the target of the short, proline-rich antibacterial peptides pyrrhocoricin, drosocin, and apidaecin (*48*, *49*). Apparently, pyrrhocoricin inhibits both DnaK-mediated ATP hydrolysis and protein refolding. Direct binding studies showed that these proline-rich antibiotics bind to the αD and αE helices of DnaK (*50*). We have shown here that these two key helices are crucial for "lid stability", where lid stability is defined as the ability of the lid, depending on the presence or absence of key helices, to be an unraveled internal ligand or an antiparallel helical bundle. If the deletion of the αE helix can have such a profound effect on ATP binding (Table 1), it certainly is reasonable that the binding of an exogenous molecule, such as pyrrhocoricin, to the αD+αE helices could change the conformation of the lid, resulting in dramatic changes in the kinetics of the DnaK reaction cycle.

In summary, the αD and αE helices are key helices for lid stability. When a substrate is bound in the substrate-binding domain of DnaK, the αD helix is necessary and sufficient for the formation of the antiparallel helical bundle composed of helices B, C, and D. This three-helical bundle interacts with and stabilizes the β-sandwich via the latch (Figure 7A), creating long-lived DnaK−peptide complexes. One possibility is that the αD helix promotes formation of the αB−αD helical bundle through the two residues, E590 and L591, which are conserved between *E. coli* DnaK, bovine Hsc70, and hamster Bip. Notice that the side-chains of these two residues flank, and thus perhaps stabilize, αC (Figure 7A). Another possibility is that the αD helix promotes formation of the αB−αD helical bundle via a salt bridge between E531 and K581, which are residues of αB and αD (Figure 7A,B), respectively. We are currently making point mutations in DnaK to determine how the αD helix stabilizes the lid and how the flexible subdomain modulates ATP binding.

ACKNOWLEDGMENT

We thank Dr. Donard Dwyer for preparing the structure figure.

REFERENCES

1. Witt, S. N., and Slepenkov, S. V. (1999) *J. Fluoresc. 9*, 281−293.
2. Bukau, B., and Horwich, A. L. (1998) *Cell 92*, 351−366.
3. Hartl, F. U., and Hayer-Hartl, M. (2002) *Science 295*, 1852−8.
4. Zylicz, M., Ang, D., and Georgopoulos, C. (1987) *J. Biol. Chem. 262*, 17437−17442.
5. Liberek, K., Marszalek, J., Ang, D., Georgopoulos, C., and Zylicz, M. (1991) *Proc. Natl. Acad. Sci. U.S.A. 88*, 2874−2878.
6. Packschies, L., Theyssen, H., Bucherberger, A., Bukau, B., Goody, R. S., and Reinstein, J. (1997) *Biochemistry 36*, 3417−3422.
7. Karzai, A. W., and McMacken, R. (1996) *J. Biol. Chem. 271*, 11236−11246.
8. Russell, R., Karzai, A. W., Mehl, A. F., and McMacken, R. (1999) *Biochemistry 38*, 4165−4176.
9. Flaherty, K. M., DeLuca-Flaherty, C., and McKay, D. B. (1990) *Nature 346*, 623−628.
10. Harrison, C. J., Hayer-Hartl, M., Di Liberto, M., Hartl, F.-U., and Kuriyan, J. (1997) *Science 276*, 431−435.
11. Morshauser, R. C., Wang, H., Glynn, G. C., and Zuiderweg, R. P. (1995) *Biochemistry 34*, 6261−6266.
12. Zhu, X., Zhao, X., Burkholder, W. F., Gragerov, A., Ogata, C. M., Gottesman, M. E., and Hendrickson, W. A. (1996) *Science 272*, 1606−1614.
13. Pellecchia, M., Montgomery, D. L., Stevens, S. Y., Vander Kooi, C. W., Feng, H.-P., Gierasch, L. M., and Zuiderweg, E. R. P. (2000) *Nat. Struct. Biol. 7*, 298−303.
14. Mayer, M., Schroder, H., Rudiger, S., Paal, K., Laufen, T., and Bukau, B. (2000) *Nat. Struct. Biol. 7*, 586−593.
15. Buczynski, G., Slepenkov, S. V., Sehorn, M. G., and Witt, S. N. (2001) *J. Biol. Chem. 276*, 27231−27236.
16. Bertelsen, E. B., Zhou, H., Lowry, D. F., Flynn, G. C., and Dahlquist, F. W. (1999) *Protein Sci. 8*, 343−54.
17. Qian, X., Hou, W., Zhengang, L., and Sha, B. (2002) *Biochem. J. 361*, 27−34.
18. Slepenkov, S. V., and Witt, S. N. (2002) *Biochemistry 41*, 12224−12235.
19. Farr, C. D., Galiano, F. J., and Witt, S. N. (1995) *Biochemistry 34*, 15574−15582.
20. Slepenkov, S. V., and Witt, S. N. (1998) *Biochemistry 37*, 1015−1024.
21. Gao, B., Greene, L., and Eisenberg, E. (1994) *Biochemistry 33*, 2048−2054.
22. Schmid, D., Baici, A., Gehring, H., and Christen, P. (1994) *Science 263*, 971−973.
23. Pierpaoli, E. V., Sanmeier, E., Baici, A., Schönfeld, H.-J., Gisler, S., and Christen, P. (1997) *J. Mol. Biol. 269*, 757−768.
24. Bukau, B., and Walker, G. C. (1989) *J. Bacteriol. 171*, 6030−6038.
25. Laemmli, U. K. (1970) *Nature 227*, 680−685.
26. Slepenkov, S. V., and Witt, S. N. (1998) *Biochemistry 37*, 16749−16756.
27. Bevington, P. R. (1969) *Data Reduction and Error Analysis for the Physical Sciences*, McGraw-Hill, New York.
28. Bardwell, J. C., Tilly, K., Craig, E., King, J., Zylicz, M., and Georgopoulos, C. (1986) *J. Biol. Chem. 261*, 1782−1785.
29. Bernasconi, C. F. (1976) *Relaxation Kinetics*, Academic Press, New York.
30. Wang, H., Kurochkin, A. V., Pang, Y., Hu, W., Flynn, G. C., and Zuiderweg, E. R. P. (1998) *Biochemistry 37*, 7929−7940.
31. Flynn, G. C., Chappell, T. G., and Rothman, J. E. (1989) *Science 245*, 385−390.

32. Jordan, R., and McMacken, R. (1995) *J. Biol. Chem. 270*, 4563−4569.
33. Russell, R., Jordan, R., and McMacken, R. (1998) *Biochemistry 37*, 596−607.
34. Farr, C. D., Slepenkov, S. V., and Witt, S. N. (1998) *J. Biol. Chem. 273*, 9744−9748.
35. Gisler, S. M., Pierpaoli, E. V., and Christen, P. (1998) *J. Mol. Biol. 279*, 833−840.
36. Pierpaoli, E. V., Gisler, S. M., and Christen, P. (1998) *Biochemistry 37*, 16741−16748.
37. Buchberger, A., Theyssen, H., Schroder, H., McCarty, J. S., Virgallita, G., Milkereit, P., Reinstein, J., and Bukau, B. (1995) *J. Biol. Chem. 270*, 16903−16910.
38. Ha, J.-H., and McKay, D. B. (1994) *Biochemistry 33*, 14625−14635.
39. Wilbanks, S. M., Chen, L., Tsuruta, H., Hodgson, K. O., and McKay, D. B. (1995) *Biochemistry 34*, 12095−12106.
40. Shi, L., Kataoka, M., and Fink, A. L. (1996) *Biochemistry 35*, 3297−3308.
41. Ha, J.-H., and McKay, D. B. (1995) *Biochemistry 34*, 11635−11644.
42. Theyssen, H., Schuster, H.-P., Packschies, L., Bukau, B., and Reinstein, J. (1996) *J. Mol. Biol. 263*, 657−670.
43. Hiromi, K. (1979) *Kinetics of Fast Enzyme Reactions. Theory and Practice.* John Wiley & Sons, New York.
44. Schönfeld, H.-J., Schmidt, D., Schröder, H., and Bukau, B. (1995) *J. Biol. Chem. 270*, 2183-2189.
45. Freeman, B. C., Myers, M. P., Schumacher, R., and Morimoto, R. I. (1995) *EMBO J. 14*, 2281−92.
46. Anderson, C. M., Stenkamp, R. E., McDonald, R. C., and Steitz, T. A. (1978) *J. Mol. Biol. 123*, 207−219.
47. Hoggett, J. G., and Kellett, G. L. (1995) *Biochem. J. 305*, 405−410.
48. Otvos, L., Jr., O, I., Rogers, M. E., Consolvo, P. J., Condie, B. A., Lovas, S., Bulet, P., and Blaszczyk-Thurin, M. (2000) *Biochemistry 39*, 14150−9.
49. Kragol, G., Lovas, S., Varadi, G., Condie, B. A., Hoffmann, R., and Otvos, L., Jr. (2001) *Biochemistry 40*, 3016−26.
50. Kragol, G., Hoffmann, R., Chattergoon, M. A., Lovas, S., Cudic, M., Bulet, P., Condie, B. A., Rosengren, K. J., Montaner, L. J., and Otvos, L., Jr. (2002) *Eur. J. Biochem. 269*, 4226−37.

BI034126V